

Euler Class Topological Insulators

Theory and Numerical Results for Multi-Band Models

Debanjan Sinha Mahapatra(IISER KOLKATA)

Supervisor : Adrien Bouhon(NORDITA)

September 28, 2025

Outline

Foundations Theoretical Framework

Results I: k.p Analysis of 3-Band Models

Results II: Bulk-Boundary Correspondence in a 4-Band Model

Outlook

Foundations Theoretical Framework

Historical Perspective

- 1980s: Quantum Hall Effect showed that a physical quantity could be perfectly quantized, explained by a topological invariant (**Chern Number**).

Historical Perspective

- 1980s: Quantum Hall Effect showed that a physical quantity could be perfectly quantized, explained by a topological invariant (**Chern Number**).
- 2005–2007: The field exploded with the discovery of **\mathbb{Z}_2 Topological Insulators**, protected by time-reversal symmetry.

Historical Perspective

- 1980s: Quantum Hall Effect showed that a physical quantity could be perfectly quantized, explained by a topological invariant (**Chern Number**).
- 2005–2007: The field exploded with the discovery of \mathbb{Z}_2 **Topological Insulators**, protected by time-reversal symmetry.
- 2017–Present: The frontier moved to classifying more subtle phases, leading to the concepts of **higher-order** and **fragile topology**.

The Bulk-Boundary Correspondence (Chern Case)

- A non-trivial bulk invariant
forces gapless states at a boundary with a trivial vacuum.

The Bulk-Boundary Correspondence (Chern Case)

- A non-trivial bulk invariant **forces** gapless states at a boundary with a trivial vacuum.
- The bulk Hall conductivity is quantized by the Chern number C :

$$\sigma_{xy} = C \frac{e^2}{h}$$

The Bulk-Boundary Correspondence (Chern Case)

- A non-trivial bulk invariant forces gapless states at a boundary with a trivial vacuum.
- The bulk Hall conductivity is quantized by the Chern number C :

$$\sigma_{xy} = C \frac{e^2}{h}$$

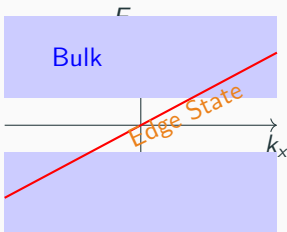
- This bulk property dictates that there must be C conducting 1D channels (edge states) at the boundary.

The Bulk-Boundary Correspondence (Chern Case)

- A non-trivial bulk invariant **forces** gapless states at a boundary with a trivial vacuum.
- The bulk Hall conductivity is quantized by the Chern number C :

$$\sigma_{xy} = C \frac{e^2}{h}$$

- The gap must close at the edge to support these states.



- This bulk property dictates that there must be C conducting 1D channels (edge states) at the boundary.

The Role of Symmetry in Band Theory

Symmetry constrains the form of the Hamiltonian and the wavefunctions.

- A tight-binding model can be Fourier transformed into the Bloch picture:

$$\hat{H} = \sum_{\mathbf{k} \in BZ} \sum_{\alpha, \beta} |\phi_{\alpha, \mathbf{k}}\rangle H_{\alpha\beta}(\mathbf{k}) \langle \phi_{\beta, \mathbf{k}}|$$

The Role of Symmetry in Band Theory

Symmetry constrains the form of the Hamiltonian and the wavefunctions.

- A tight-binding model can be Fourier transformed into the Bloch picture:

$$\hat{H} = \sum_{\mathbf{k} \in BZ} \sum_{\alpha, \beta} |\phi_{\alpha, \mathbf{k}}\rangle H_{\alpha\beta}(\mathbf{k}) \langle \phi_{\beta, \mathbf{k}}|$$

- **C_2T symmetry** is an anti-unitary symmetry $\mathcal{A} = UK$ that is crucial for real topological phases. It satisfies:

$$\mathcal{A}^2 = +1 \implies \text{no Kramer's degeneracies}$$

The Role of Symmetry in Band Theory

Symmetry constrains the form of the Hamiltonian and the wavefunctions.

- A tight-binding model can be Fourier transformed into the Bloch picture:

$$\hat{H} = \sum_{\mathbf{k} \in BZ} \sum_{\alpha, \beta} |\phi_{\alpha, \mathbf{k}}\rangle H_{\alpha\beta}(\mathbf{k}) \langle \phi_{\beta, \mathbf{k}}|$$

- C_2T symmetry is an anti-unitary symmetry $\mathcal{A} = UK$ that is crucial for real topological phases. It satisfies:

$$\mathcal{A}^2 = +1 \implies \text{no Kramer's degeneracies}$$

- **Key Consequence:** Within a plane left invariant by the symmetry (the C_2T plane), the Hamiltonian is forced to be **real and symmetric**:

$$\mathbf{1} \cdot \tilde{H}^*(\mathbf{k}) \cdot \mathbf{1} = \tilde{H}(\mathbf{k})$$

This reality condition makes the Chern number vanish and the **Euler class** the relevant invariant.

The Euler Class: Topology of Real Bundles

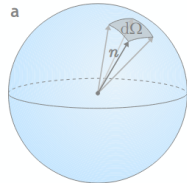
Chern Class (Complex Case)

- Describes complex vector bundles.
- Hamiltonian: $H(\mathbf{k}) = \mathbf{h}(\mathbf{k}) \cdot \boldsymbol{\sigma}$
- Curvature: $F_{ij} = \frac{1}{2}\mathbf{n} \cdot (\partial_i \mathbf{n} \times \partial_j \mathbf{n})$
- Invariant: $c_1 \in \mathbb{Z}$

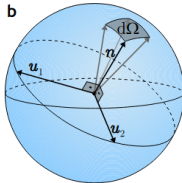
Euler Class (Real Case, $C_2 T^2 = +1$)

- Describes real oriented vector bundles.
- Hamiltonian: $H(\mathbf{k}) = 2\mathbf{n}\mathbf{n}^T - 1$
- Euler Form: $Eu_{ij} = \mathbf{n} \cdot (\partial_i \mathbf{n} \times \partial_j \mathbf{n})$
- Invariant: $\chi \in 2\mathbb{Z}$

$$c_1 \in \mathbb{Z}$$



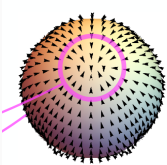
$$\chi \in 2\mathbb{Z}$$



Euler Class from Nodal Points Patches

Nodal Points Vortices:

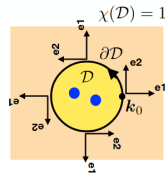
- Per the Poincaré-Hopf theorem, the Euler class is the sum of the vorticities (winding numbers) of the vector field $\mathbf{n}(\mathbf{k})$ around its zeros.
- These zeros are the **nodal points** between bands.
- The number of stable nodal points is directly related to the Euler class: $\#NP = 2|\chi|$.



Patch Euler Number:

- The total Euler class can be computed by summing the local contributions from patches \mathcal{D}_n around each nodal point.

$$\begin{aligned}\chi(\mathcal{D}) &= \frac{1}{\pi} \sum_n \left[\int_{\mathcal{D}_n} Eu - \oint_{\partial\mathcal{D}_n} a \right] \\ &= \sum_n W_n \in \mathbb{Z}\end{aligned}$$



Results I: k.p Analysis of 3-Band Models

$k \cdot p$ Expansion of the Square Lattice Model

Method:

- Start with a 3-band tight-binding Hamiltonian on the square lattice.
- Perform a $k \cdot p$ expansion around the Γ point to get a low-energy effective Hamiltonian.

$k \cdot p$ Expansion of the Square Lattice Model

Method:

- Start with a 3-band tight-binding Hamiltonian on the square lattice.
- Perform a $k \cdot p$ expansion around the Γ point to get a low-energy effective Hamiltonian.

Model Hamiltonian:

$$H = \begin{pmatrix} -\frac{9}{4} + s_1^2 & s_1 s_2 & (1 - c_1 - c_2)s_1 \\ s_1 s_2 & \frac{7}{4} + s_2^2 & (1 - c_1 - c_2)s_2 \\ (1 - c_1 - c_2)s_1 & (1 - c_1 - c_2)s_2 & -2 + (c_1 + c_2 - 1)^2 \end{pmatrix}$$

where $c_i = \cos(\pi k_i)$, $s_i = \sin(\pi k_i)$

k.p Expansion of the Square Lattice Model

Method:

- Start with a 3-band tight-binding Hamiltonian on the square lattice.
- Perform a k·p expansion around the Γ point to get a low-energy effective Hamiltonian.

Model Hamiltonian:

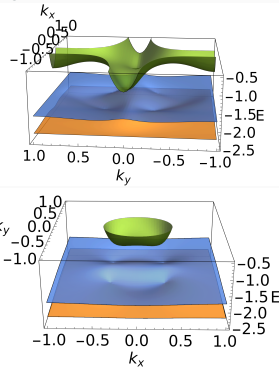
$$H = \begin{pmatrix} -\frac{9}{4} + s_1^2 & s_1 s_2 & (1 - c_1 - c_2) s_1 \\ s_1 s_2 & \frac{7}{4} + s_2^2 & (1 - c_1 - c_2) s_2 \\ (1 - c_1 - c_2) s_1 & (1 - c_1 - c_2) s_2 & -2 + (c_1 + c_2 - 1)^2 \end{pmatrix}$$

where $c_i = \cos(\pi k_i)$, $s_i = \sin(\pi k_i)$

k.p Approximated Hamiltonian:

$$H_{kp} = \begin{pmatrix} -\frac{9}{4} + k_1^2 \pi^2 & k_1 k_2 \pi^2 & \frac{k_1 \pi}{2} (-2 + \pi^2 (k_1^2 + k_2^2)) \\ k_1 k_2 \pi^2 & \frac{7}{4} + k_2^2 \pi^2 & \frac{k_2 \pi}{2} (-2 + \pi^2 (k_1^2 + k_2^2)) \\ \frac{k_1 \pi}{2} (\dots) & \frac{k_2 \pi}{2} (\dots) & -2 + \frac{1}{4} (-2 + \pi^2 (k_1^2 + k_2^2))^2 \end{pmatrix}$$

Original vs. Perturbed Spectrum:



Euler Form of the Square Lattice Model

The Euler Form:

- The Euler form is the integrand of the Euler class ($\chi = \frac{1}{2\pi} \int \mathbf{e} d^2k$).
- It can be viewed as the density of "topological charge" in the Brillouin zone.
- Its peaks indicate the momentum-space regions that contribute most to the non-trivial topology.

Plotting the Euler form inside the rectangle...

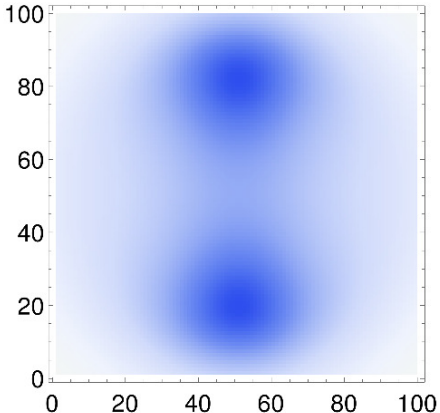


Figure: Euler form for the gapped square lattice model, showing strong peaks that integrate to $\chi = 2$.

k.p Expansion of the Kagome Lattice Model

Method:

- Apply k·p expansion to a 3-band Kagome lattice model.

k.p Expansion of the Kagome Lattice Model

Method:

- Apply k·p expansion to a 3-band Kagome lattice model.

Model Hamiltonian:

$$H = \begin{pmatrix} \frac{4}{5}c_1 & c_{1-2} + c_{1+2} & c_2 + c_{21+2} \\ c_{1-2} + c_{1+2} & \frac{4}{5}c_2 & c_1 + c_{1+22} \\ c_2 + c_{21+2} & c_1 + c_{1+22} & \frac{4}{5}c_{1+2} \end{pmatrix}$$

where $c_i = \cos(\pi k_i)$, $c_{1\pm 2} = \cos(\frac{\pi}{2}(k_1 \pm k_2))$,
etc.

$k\cdot p$ Expansion of the Kagome Lattice Model

Method:

- Apply $k\cdot p$ expansion to a 3-band Kagome lattice model.

Model Hamiltonian:

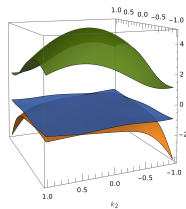
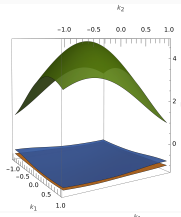
$$H = \begin{pmatrix} \frac{4}{5}c_1 & c_{1-2} + c_{1+2} & c_2 + c_{21+2} \\ c_{1-2} + c_{1+2} & \frac{4}{5}c_2 & c_1 + c_{1+22} \\ c_2 + c_{21+2} & c_1 + c_{1+22} & \frac{4}{5}c_{1+2} \end{pmatrix}$$

where $c_i = \cos(\pi k_i)$, $c_{1\pm 2} = \cos(\frac{\pi}{2}(k_1 \pm k_2))$,
etc.

$k\cdot p$ Approximated Hamiltonian:

$$H_{kp} = \begin{pmatrix} \frac{4}{5}(1 - \frac{\pi^2 k_1^2}{2}) & 2 - \frac{\pi^2(k_1^2 + k_2^2)}{4} & \dots \\ 2 - \frac{\pi^2(k_1^2 + k_2^2)}{4} & \frac{4}{5}(1 - \frac{\pi^2 k_2^2}{2}) & \dots \\ \dots & \dots & \frac{4}{5}(1 - \frac{\pi^2(k_1 + k_2)^2}{2}) \end{pmatrix}$$

Original vs. Perturbed Spectrum:



Euler Form of the Kagome Lattice Model

Topological Charge:

- The Euler form for the Kagome model shows a different distribution of topological charge.
- The integral confirms the Euler class is $\chi = 1$.
- This confirms k·p theory is a valid tool for analyzing fragile topology in different geometries.

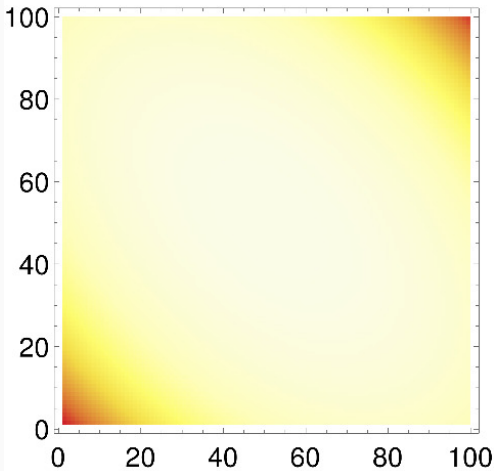


Figure: Euler form for the gapped Kagome model. The charge is concentrated near the BZ corners.

Results II: Bulk-Boundary Correspondence in a 4-Band Model

The 4-Band Model: Bulk Properties

Model Hamiltonian $H(k_1, k_2)$:

$$\begin{pmatrix} s_2 & s_1 & -1/4 & 1 - c_1 - c_2 \\ s_1 & -s_2 & -1 + c_1 + c_2 & 1/4 \\ -1/4 & -1 + c_1 + c_2 & s_2 & s_1 \\ 1 - c_1 - c_2 & 1/4 & s_1 & -s_2 \end{pmatrix}$$

where $c_i = \cos(k_i \pi)$, $s_i = \sin(k_i \pi)$

The 4-Band Model: Bulk Properties

Model Hamiltonian $H(k_1, k_2)$:

$$\begin{pmatrix} s_2 & s_1 & -1/4 & 1 - c_1 - c_2 \\ s_1 & -s_2 & -1 + c_1 + c_2 & 1/4 \\ -1/4 & -1 + c_1 + c_2 & s_2 & s_1 \\ 1 - c_1 - c_2 & 1/4 & s_1 & -s_2 \end{pmatrix}$$

where $c_i = \cos(k_i \pi)$, $s_i = \sin(k_i \pi)$

Bulk Analysis:

- A Wilson loop calculation confirms the model has a **non-trivial bulk invariant**.
- The 3D bulk band structure shows the system is fully gapped.

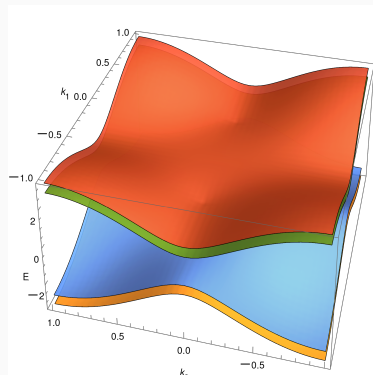


Figure: 3D Bulk Spectrum.

Ribbon Spectrum 1D Edge States

Method:

- Simulation on a ribbon geometry (open boundaries in one direction).

Ribbon Spectrum 1D Edge States

Method:

- Simulation on a ribbon geometry (open boundaries in one direction).

Result:

- The bulk gap hosts new in-gap states.

Ribbon Spectrum 1D Edge States

Method:

- Simulation on a ribbon geometry (open boundaries in one direction).

Result:

- The bulk gap hosts new in-gap states.

Interpretation:

- These are the **1D edge states** predicted by the non-trivial bulk. They are the first signature of the bulk-boundary correspondence.

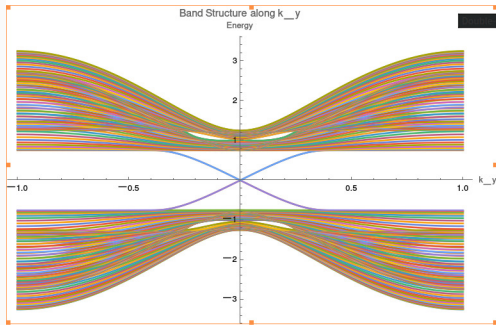


Figure: Ribbon spectrum showing protected 1D edge states crossing the bulk gap.

Finite Flake Simulation Corner States

Method:

- We simulate a 2D ribbon of the 4-band model, finite in x direction , infinite and periodic in y direction

Finite Flake Simulation Corner States

Method:

- We simulate a 2D ribbon of the 4-band model, finite in x direction , infinite and periodic in y direction

Result:

- The low-energy states show a remarkable concentration of their probability density $|\psi|^2$ at the edges.

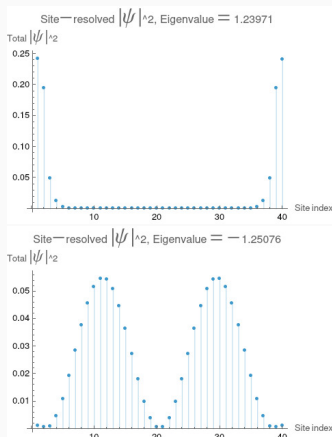


Figure: The resolved site $|\psi|^2$ shows a clear localization at the edges of the system (with 40 sites)

Outlook

Conclusion

- We have analyzed fragile topology in multi-band models using both analytical $k \cdot p$ theory and full numerical simulations.

Conclusion

- We have analyzed fragile topology in multi-band models using both analytical $k \cdot p$ theory and full numerical simulations.
- **$k \cdot p$ Theory:** Successfully captures the integer Euler class invariant ($\chi = 2$ for square, $\chi = 1$ for Kagome) in low-energy models.

Conclusion

- We have analyzed fragile topology in multi-band models using both analytical $k \cdot p$ theory and full numerical simulations.
- **$k \cdot p$ Theory:** Successfully captures the integer Euler class invariant ($\chi = 2$ for square, $\chi = 1$ for Kagome) in low-energy models.
- **4-Band Model:** Provides a complete demonstration of the higher-order bulk-boundary correspondence, from the gapped bulk to 1D edge states and finally to localized 0D corner modes.

Conclusion

- We have analyzed fragile topology in multi-band models using both analytical $k \cdot p$ theory and full numerical simulations.
- **$k \cdot p$ Theory:** Successfully captures the integer Euler class invariant ($\chi = 2$ for square, $\chi = 1$ for Kagome) in low-energy models.
- **4-Band Model:** Provides a complete demonstration of the higher-order bulk-boundary correspondence, from the gapped bulk to 1D edge states and finally to localized 0D corner modes.
- **Outlook:** This work validates the theoretical framework of fragile topology and provides tools to identify and engineer these phases in real materials and metamaterials.

References i

-  W. A. Benalcazar, B. A. Bernevig, T. L. Hughes.
Quantized electric multipole insulators.
Science 357, 61-66 (2017).
-  F. Schindler, A. M. Cook, M. G. Vergniory, et al.
Higher-order topological insulators.
Science Advances 4, eaat0346 (2018).
-  B. Bradlyn, L. Elcoro, J. Cano, et al.
Topological quantum chemistry.
Nature 547, 298–305 (2017).